www.czasopisma.pan.pl PAN POLSKA AKADEMIA NAUK www.journals.pan.pl

Arch. Metall. Mater. **66** (2021), 4, 1115-1121

DOI: 10.24425/amm.2021.136431

RIRIN EVA HIDAYATI[1], FITRIA SANDI FARADILLA[1], DADANG DADANG[1], LIA HARMELIA[1], NURLINA NURLINA[2], DIDIK PRASETYOKO[1], HAMZAH FANSURI[1*]

# SETTING TIME AND COMPRESSIVE STRENGTH OF GEOPOLYMERS MADE OF THREE INDONESIAN LOW CALCIUM FLY ASH WITH VARIATION OF SODIUM SILICATE ADDITION

In this research, the effect of sodium silicate ($Na_2SiO_3$) on the geopolymerization of fly ash type F (low calcium) has been studied. The variations of $Na_2SiO_3$ used in the synthesized geopolymers were 19, 32, and 41wt%. The fly ash from three different power plant sources was characterized using X-Ray Fluorescence (XRF), X-Ray Diffraction (XRD), Particle Size Analyzer (PSA), and Scanning Electron Microscopy (SEM). Fly ash-based geopolymers were tested for mechanical strength and setting time. The best geopolymer was obtained by adding 32% $Na_2SiO_3$, produced a compressive strength of 21.62 MPa with a setting time of 30 hours. Additions of 19wt% $Na_2SiO_3$ failed to form geopolymer paste while the addition of 41wt% $Na_2SiO_3$ decreased the mechanical strength of the geopolymer. Higher calcium content in low calcium fly ash produces stronger geopolymer and faster setting time.

*Keywords:* Fly ash, geopolymer, sodium silicate, low calcium, waste management

## 1. Introduction

Geopolymer refers to the condensation product of aluminate and silicate ions to form three-dimensional amorphous aluminosilicate networks. Geopolymers can be made from various aluminosilicate materials. At the beginning of the development of geopolymers, Davidovits used kaolin as an aluminosilicate source while sodium silicate and NaOH solution were used as activating agents [1-5]. Fly ash is one of the coal combustion by-products that contain aluminosilicate materials. It has caught the high attention of researchers in recent decades due to the steady increase of fly ash production as the demand for electricity and coal consumption increases [1-3]. The utilization of fly ash is focused on large-scale applications, such as geopolymer, building materials, road construction, filler, and agriculture [5-10].

In geopolymer application, the physical and chemical properties of fly ash, which depends on the type of coal used and the combustion process in the power plant, affect the geopolymerization process. The physical properties refer to particle size and distribution; crystallinity, and morphology, while the chemical properties refer to chemical components and composition. One of the chemical properties that affect the geopolymerization reaction is calcium content. Fly ash with high calcium content produces geopolymers with fast setting time and a fairly high and stable initial mechanical strength. On the other hand, fly ash with low calcium will produce very low setting time or even fails to geopolymerize.

Zhang et al. [11] reported that the important factors that influence the fly ash geopolymerization process are water content, activating bases, types of cations in the activating bases, morphology, and crystallinity. The process requires strong alkalis to activate Si and Al from fly ash [12]. In addition to NaOH as a strong alkali to activate fly ash, geopolymerization also requires the addition of soluble silicates in the liquid phase, so the activated silicates of fly ash can react with soluble silicate additive in the polycondensation at an early stage [13]. Sodium silicate ($Na_2SiO_3$) can also act as a binder for aluminosilicate sources. The silicate ions contained in sodium silicate are already in the form of oligomers that are ready to polymerize with silicate and aluminate ions. Therefore, the presence of sodium silicate is very important and influences important properties of geopolymer products such as compressive strength and setting time. Theoretically, the more sodium silicate is added, the more soluble silicates ions are available to react with dissolved silicates and/or aluminates of fly ash in the liquid phase of the

[1] INSTITUT TEKNOLOGI SEPULUH NOPEMBER, DEPARTMENT OF CHEMISTRY, FACULTY OF SCIENCE AND DATA ANLYTICS, KAMPUS ITS SUKOLILO, SURABAYA 60111, INDONESIA
[2] UNIVERSITAS TANJUNGPURA, FACULTY OF MATHEMATICS AND NATURAL SCIENCES, DEPARTMENT OF CHEMISTRY, PONTIANAK 78111, INDONESIA

* Corresponding author: h.fansuri@chem.its.ac.id

geopolymerization process which will gradually produce mono silicate, trimer, and cyclic chains, then form a three-dimensional polymer complex structure. The complex structure of the geopolymer matrix is responsible for the increase of mechanical properties of the geopolymer because it forms a more homogeneous microstructure [14,15].

In this work, fly ash type F from three different sources was used to produce geopolymers and the addition of sodium silicate was varied. A preliminary study showed that the fly ashes contain CaO of less than 10%. According to some reports, fly ash is classified as low in calcium if it contains less than 10% CaO [16-18]. Fly ash in this study was taken from three power plants namely Ketapang, Sanggau, and Wilmar. Based on our early study, these fly ashes failed to form geopolymers when they were made under a standardized method [19]. There are some reasons behind the unsuccessful geopolymerization of the three low calcium fly ash, one of which is the lack of sodium silicate to form oligomers which will later become the initiator of the geopolymerization reaction. In addition to sodium silicate, low calcium content can also cause a slow setting time of geopolymer. Therefore, it is necessary to observe the effect of sodium silicate amount in the preparation of geopolymers using low calcium fly ash and study their effect on mechanical strength and setting time of geopolymer products.

## 2. Method

### 2.1. Materials

Three different sources of fly ash were used for this research. They were collected from Ketapang, Sanggau, and Wilmar Power Plant. Ketapang and Sanggau are located in West Kalimantan while Wilmar is located in East Java, Indonesia. Pro analytical grade chemicals aluminum hydroxide ($Al(OH)_3$) powder and sodium hydroxide (NaOH) pellets of Sigma-Aldrich while technical grade sodium silicate ($Na_2SiO_3$) of PT. Brataco was used as an additive and alkaline activator.

### 2.2. Fly ash preparation

All fly ashes were firstly sieved using a 100-mesh test sieve and dried in an oven at 105°C for 24 hours. The dried ash was then characterized using XRF, XRD, SEM, and PSA. XRF (X-Ray Fluorescence) was used to determine the elemental composition of the ashes. The XRF instrument used was the XRF spectrometer S8 Tiger WD, Bruker. XRD (X-Ray Diffraction) was used to determine the crystallinity and phase composition of fly ash. The analysis was performed using the Xpert PANalytical XRD instrument, using CuKα1 (λ = 1.5406 Å) radiation and running at 40kV and 30 mA. Measurements were taken from 5 to 95° 2θ at a speed of 2° $min^{-1}$ with a step size of 0.02°. Phase identification was carried out using *Match* software. SEM (Scanning Electron Microscope, Zeiss Evo MA 10) was used to determine the morphology and shape of fly ash particles. PSA (Particle Size Analyzer, Malvern' Mastersizer 2000) was used to determine the particle size distribution of fly ash.

### 2.3. Preparation of geopolymer

Geopolymer preparation was started by mechanically mixed the sieved and dried fly ash with $Al(OH)_3$ powder. Sodium hydroxide and sodium silicate solution were added into the mixture and stirred using a hand mixer for 4 minutes to form a geopolymer paste. The sodium hydroxide solution was made one day before geopolymer preparation. The composition of chemicals used in geopolymer preparation can be seen in Table 1. Geopolymer paste was molded in cylindrical molds with a diameter to height ratio of 1:2 and leave to hardens in the air at room temperature. The hardened geopolymer was then removed from the mold, put into a plastic clip bag, and heated in an oven for 24 hours at 55°C. The geopolymer was then cured in the air at room temperature for 7 days.

TABLE 1

The composition of the raw material for making geopolymers

| Sample Name | Mass (g) | | | | Concentration of $Na_2SiO_3$ (mass %) |
|---|---|---|---|---|---|
| | Fly Ash | $Al(OH)_3$ | NaOH | $Na_2SiO_3$ | |
| Ketapang | 260 | 3.4 | 78 | 80 | 19 |
| | 260 | 3.4 | 78 | 160 | 32 |
| | 260 | 3.4 | 78 | 240 | 41 |
| Sanggau | 260 | 3.4 | 78 | 80 | 19 |
| | 260 | 3.4 | 78 | 160 | 32 |
| | 260 | 3.4 | 78 | 240 | 41 |
| Wilmar | 260 | 3.4 | 78 | 80 | 19 |
| | 260 | 3.4 | 78 | 160 | 32 |
| | 260 | 3.4 | 78 | 240 | 41 |

### 2.4. Geopolymer characterization

Setting time testing of geopolymer was carried out using a Vicat needle. The geopolymer paste in the mold was inserted with a loaded Vicat needle. The Vicat needle penetrates the geopolymer and its depth was measured. The test was repeated with a certain interval according to the consistency of the geopolymer paste and the setting time was reported as the total time needed until the loaded Vicat needle cannot penetrate the paste.

A compressive strength test of geopolymers was carried out using a universal testing machine. The test was applied to geopolymer samples after being cured for 7 days. Before the test, the top and bottom sides of geopolymer samples (cylindrical form) were flattened. Each testing was done using 5 specimens. The data obtained was the compressive force exerted on the geopolymer in kilo Newton (kN) units. The analysis results are converted and presented in Mega Pascal (MPa) units.

## 3. Result and discussion

### 3.1. Chemical composition of fly ash

The chemical composition of fly ashes, obtained by XRF, is shown in Table 2. Major chemical components are $SiO_2$ and $Al_2O_3$. The mol ratio of $SiO_2$:$Al_2O_3$ is an important factor that affects geopolymer properties [20]. The table also shows that the composition of pozzolanic compounds (a mixture of $SiO_2$, $Al_2O_3$, and $Fe_2O_3$) in the three fly ash samples is higher than 70% and the calcium content of fly ash from Ketapang, Sanggau, and Wilmar is less than 10%. Therefore, according to ASTM C618, the three fly ash samples are classified as type F [16-18]. The three fly ashes also contained quite high $Fe_2O_3$, ranging from 11 to 15%. $Fe_2O_3$ in fly ash may react with NaOH solution to form $Fe(OH)_3$. The reaction may result in lowering NaOH concentration which is needed to dissolve Si and Al on fly ash and catalyze the condensation of silicates and aluminates ions to form a geopolymer [21]. Therefore, a high concentration of $Fe_2O_3$ may have a negative effect on the quality of the geopolymer.

TABLE 2

Oxide compounds of fly ash

| Fly ash | Composition (wt%) | | | | | | | LOI |
|---|---|---|---|---|---|---|---|---|
| | $SiO_2$ | $Al_2O_3$ | $Fe_2O_3$ | CaO | MgO | $Na_2O$ | Others | |
| **Ketapang** | 40.42 | 19.45 | 13.49 | 9.31 | 5.45 | 0.51 | 11.37 | 6.59 |
| **Sanggau** | 38.09 | 23.10 | 15.17 | 8.74 | 5.50 | 0.56 | 8.84 | 4.98 |
| **Wilmar** | 51.02 | 20.80 | 11.64 | 4.70 | 1.42 | 0.26 | 10.16 | 5.79 |

### 3.2. Composition of mineral and crystalline phase of fly ash

The mineral phase composition and crystallinity of fly ash were analyzed using XRD (X-Rays Diffraction). Diffractograms of all fly ashes are depicted in Fig. 1. The three fly ashes have many sharp peaks that indicate high crystallinity. The amorphous phase was detected as a hump between 20 and 40° 2θ although they are not very clearly seen on fly ash of Wilmar and Sanggau. The presence of an amorphous phase in fly ash has a positive effect on the geopolymerization process because it can be hydrolyzed in an alkaline solution [20,22].

The mineral phases were identified using Match 3.0 software. Fig. 1 shows that fly ashes contain the same mineral phase namely quartz (Q, $SiO_2$) mullite (M, $2Al_2O_3.SiO_2$), and Calcite (C, $CaCO_3$). The minerals in each fly ash reflect the chemical composition which was detected by XRF. However, there is no-iron containing phase was detected on the diffractogram although iron content is relatively high in all fly ash. There are two possible cause for the undetected iron-containing minerals. Iron might be existing only in the amorphous phase or the concentration of iron-containing minerals is too low to be detected by the X-ray diffractometer.

Mullite, quartz and amorphous phase are the source of silicate and aluminate ions which are essentials in geopolymer formation. However, not all silicate and aluminates from mullite, quartz, and amorphous phase are activated and reacted to form geopolymer. Nevertheless, Jang et al. [20] reported that the unreacted particles of mullite and quartz may act as micro-aggregates during the geopolymerization process which was also supported by other reports [22,23].

Fig. 1 also shows that quartz is a dominant phase in all fly ashes. The highest concentration is shown by Wilmar fly ash where the $SiO_2$ content is also the highest (51.02 wt%). The lower intensity of quartz peak of Ketapang ($SiO_2$ = 40.42 wt%) than Sanggau ($SiO_2$ = 38.09) fly ash reflects that Si composition in the amorphous phase of Ketapang is higher than Sanggau fly ash. Gupta et al. [23] reported that fly ash reactivity doesn't relate linearly with quartz content since phases, especially amorphous, also have a contribution to fly ash reactivity.

In contrast to quartz, the diffraction intensity of calcite is proportional to the calcium content in each fly ash. It indicates that all calcium in each fly ash exists in the form of calcite. The calcium content in fly ash affects the setting time, microstructure, and mechanical strength [14]. Higher calcium content promotes faster setting time, denser microstructure, and higher mechanical strength. According to calcite content, the geopolymer with the fastest setting time and highest mechanical strength shall be made of Ketapang fly ash.

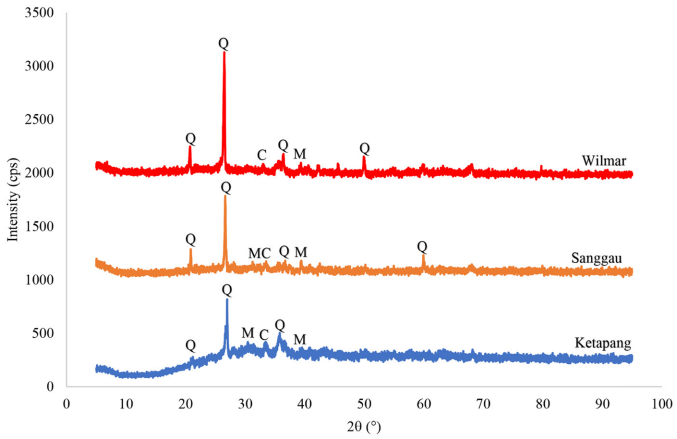


Fig. 1. X-ray diffractograms of fly ash

### 3.3. Particles size distribution of fly ash

Particle size distribution greatly affects the strength of the geopolymer. Larger fly ash particles will be more difficult to dissolve completely in an activating base solution that leads to severely incomplete geopolymerization process that affects the mechanical strength of the geopolymer product [24,25]. Therefore, it is important to characterize the particle size and size distribution of fly ash. The particle size distribution of all fly ashes is shown in Fig. 2. Fly ash of Ketapang and Sanggau have similar particle size distribution while fly ash of Wilmar has wider size distribution and higher average particle size. According to De Rossi et al. [26], the heterogeneous or non-uniform size of particles may reduce the mechanical strength of the geopolymer [26].

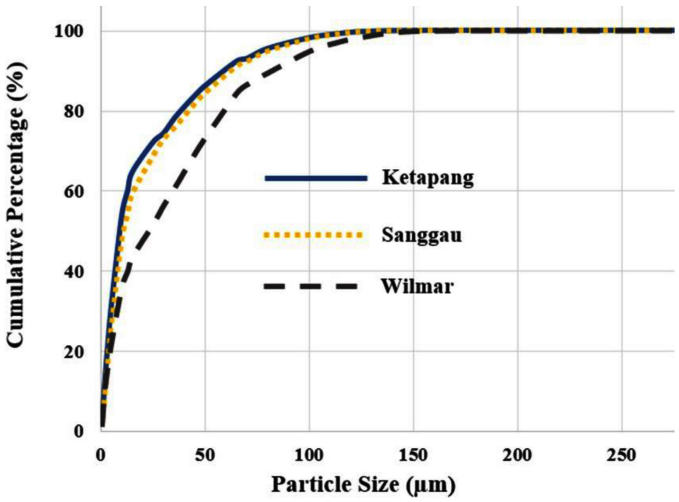


Fig. 2. Particle size distribution of fly ash

Particle size can cause different rates of geopolymerization reactions due to the dissolution process of Si and Al ions from the ash, which is started from the surface of the fly ash particles. The larger the particle size, the slower the dissolution of Si and Al ions from the fly ash. Previous reports [26-28] revealed that the small size of fly ash particles can increase the compressive strength of the geopolymer produced. Smaller particles have a larger surface area which means that more area is available to be activated by alkaline activator and then polymerized into geopolymer.

### 3.4. Morphology of fly ash

SEM analysis can be used to determine the morphology, distribution, and size of fly ash particles. Information on the shape and morphology of fly ash particles can be used to estimate the mechanical and physical properties of geopolymers [29]. SEM images in Fig. 3 shows that fly ash particles of Ketapang, Sanggau, and Wilmar are dominated by irregular shapes. A similar form was found in the results of previous studies [23,29]. Fly ash was produced from burning coal. The irregular shape of the fly ash particles indicates improper burning [23,30].

Fly ash of Ketapang has a nearly balanced particle shape between irregular and spherical particles. Fly ash of Sanggau and Wilmar were dominated by irregular shapes but the size of fly ash of Wilmar is more heterogeneous. The micrographs of all fly ashes are consistent with particle size analysis results.

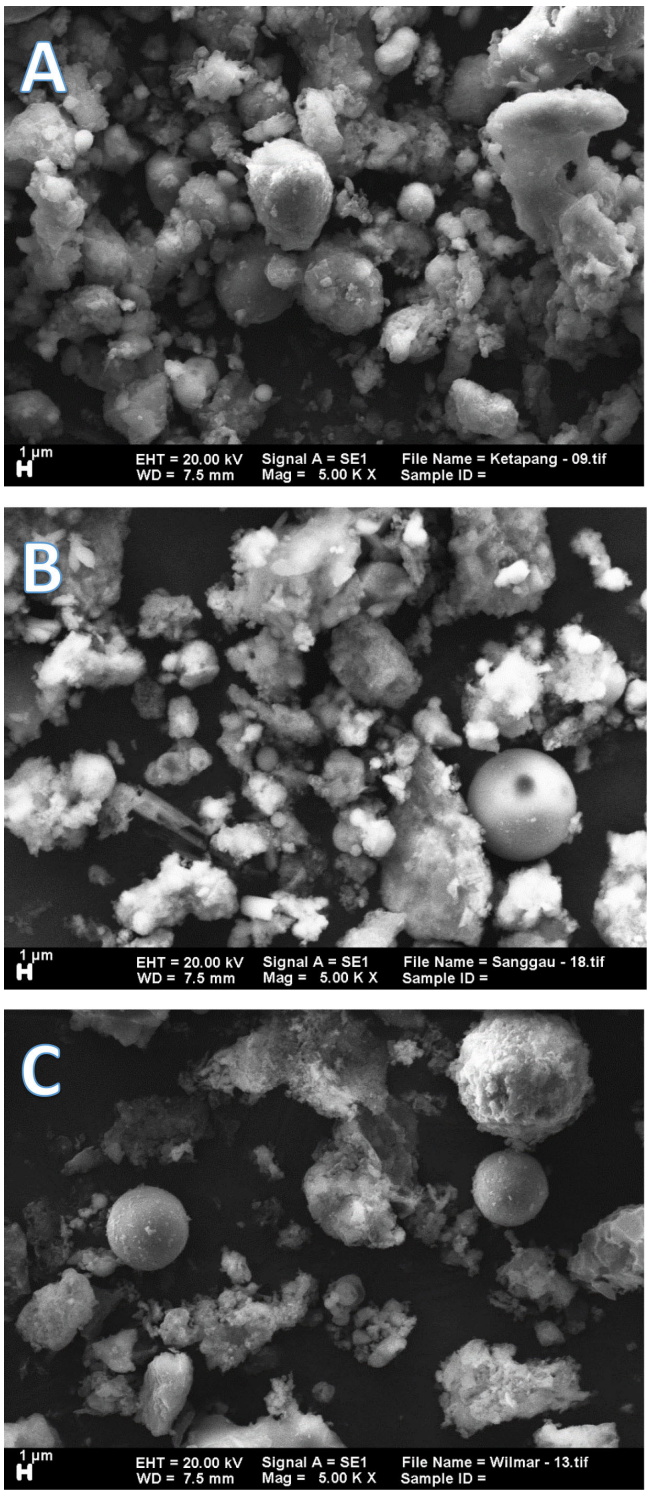


Fig. 3. SEM photo of (A) Ketapang, (B) Sanggau, (C) Wilmar fly ash

### 3.5. Setting time of geopolymer

The setting time of data geopolymer is shown in Fig. 4. Only geopolymers that were made using 19 wt% of sodium silicate failed to harden. Overall, higher sodium silicate produces a longer setting time. Geopolymer of Ketapang fly ash has the fastest setting time, followed by Sanggau and Wilmar fly ash. The sequence follows exactly the same as the calcium contents. Kaja et al. [14] explained that the presence of high calcium content in fly ash supports a faster hardening process and the formation of a geopolymer matrix and produces a denser microstructure and high mechanical strength, which affects the speed of the geopolymer setting time. The calcium content (in the form of calcite, $CaCO_3$), may react with dissolved silicate and aluminate to form calcium-aluminate-silicate-hydrate (C-A-S-H) which results in the early stage hardening [31-33]. As a result, higher calcium content produces geopolymer with a faster setting time.

Setting time of all geopolymers made of the three low calcium content fly ashes are very low compared to those reported by other researchers [27,33-35]. For example, the fastest setting time in this research is 30 hours while Zailani et al. [31] reported only 30 minutes. Fly ashes in this research contain CaO less than 10wt% while fly ash in Zailani et al. [31] was 18.4 wt%. Another factor that might alter the setting time is iron content. Fansuri et al. [36] reported that $Fe_2O_3$ can react with NaOH to form $Fe(OH)_3$ gel that consumes some NaOH so it reduces the strength of alkali activator that is needed to dissolve silicates and aluminates from fly ash and in the geopolymerization process itself. This situation might results in a reduction of setting time. However, data in Table 2 ($Fe_3O_3$ content) and Fig. 4 shows that the calcium effect is more dominant.

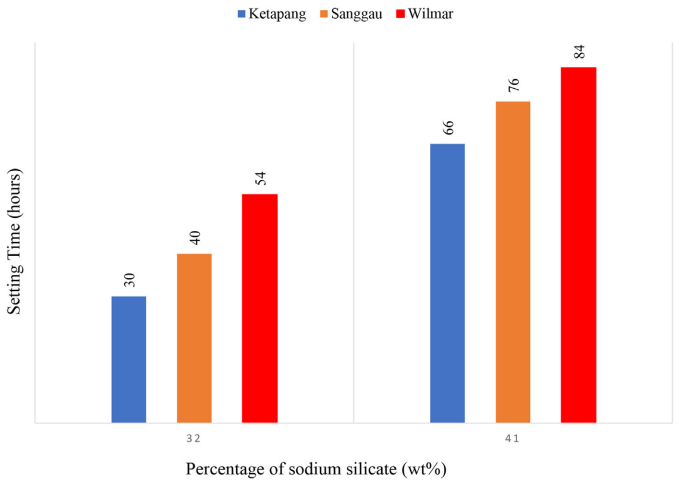


Fig. 4. Setting time of geopolymer

### 3.6. Geopolymer product and mechanical strength

Table 3 summarizes the experimental results of the geopolymerization of the three fly ashes under varied sodium silicate mass percentages. Among three variations, geopolymers made of all three fly ashes were failed to form when the added sodium silicate was 19 wt% as shown in Fig. 5. On the other hand, geopolymer pastes were formed at the addition of 32 and 41 wt% sodium silicate. Addition only 19 wt% of sodium silicate solution reduces the proportion of liquid phase in geopolymer mixture. Although the geopolymerization process produces water as a result of the condensation reaction, in the beginning, the process needs enough water to dissolve silicate and aluminate ions from fly ash and facilitating the polymerization process. Sodium silicate solution is one source of water in the geopolymerization process besides water that was intentionally added and water in the sodium oxide solution.

TABLE 3

Geopolymer synthesis observations

| Fly ash | Concentration of $Na_2SiO_3$ (wt%) | Observation Result |
|---|---|---|
| **Ketapang** | 19 | No geopolymer formed |
| | 31 | Geopolymer was formed |
| | 41 | Geopolymer was formed |
| **Sanggau** | 19 | No geopolymer formed |
| | 31 | Geopolymer was formed |
| | 41 | Geopolymer was formed |
| **Wilmar** | 19 | No geopolymer formed |
| | 31 | Geopolymer was formed |
| | 41 | Geopolymer was formed |

Fig. 6 shows the compressive strength, the sole mechanical strength test that was carried out in this research, of geopolymers of Ketapang, Sanggau, and Wilmar fly ashes. The compressive strength data of 19 wt% sodium silicate addition is not available because the geopolymer paste failed to form. The addition of 32 wt% sodium silicate resulted in the greatest compressive strength (21.62 MPa), followed by 12.08 and 8.90 MPa for geopolymer of Ketapang, Sanggau, and Wilmar fly ash, respectively. This is due to the combination of the activating bases, the amount of fly ash, and sodium silicate at the right ratio.

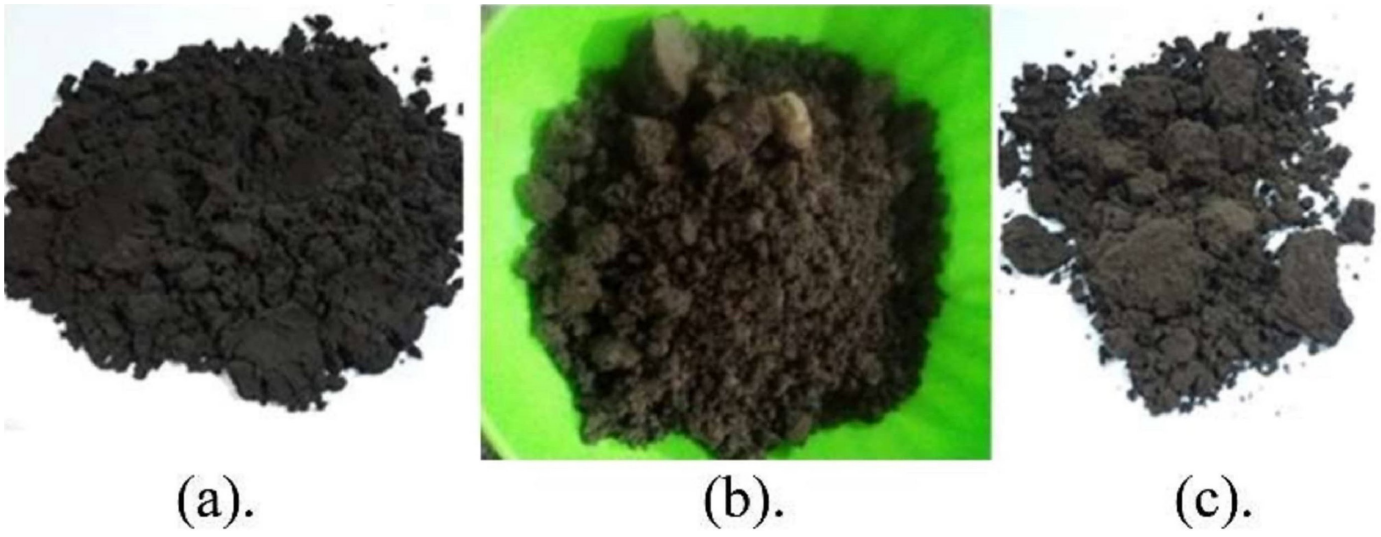


Fig. 5. Fly ash: a). Ketapang, (b). Sanggau and (c). Wilmar which failed to form geopolymers

The addition of less sodium silicate cannot form a geopolymer paste apart from the lack of viscosity produced as well as the insufficient number of activating bases to bind the fly ash. On the other hand, the addition of 41 wt% sodium silicate results in a decrease in the compressive strength of the geopolymer product. Higher sodium silicate means higher water content in the geopolymerization process. Geopolymer is produced in the gel phase. When the liquid phase is too high, the concentration of water is too high as well and hindered the formation of the gel. High water content promotes the formation of zeolite which is crystalline and may reduce the strength of geopolymer. The results show that the concentration of sodium silicate in geopolymer preparation from fly ash affects the mechanical strength of the produced geopolymer. Therefore, it is very important to control sodium silicate content in making geopolymer, particularly from low calcium fly ash.

In addition to sodium silicate, the compressive strength of geopolymer also follows the composition of calcium in the ash. Fig. 6 shows that fly ash of Ketapang with the addition of 32 wt% sodium silicate has the highest initial mechanical strength than the others due to its highest CaO content. When compressive strength as a function of sodium silicate percentage was plot together with CaO, $Fe_2O_3$, and calcite content as presented in Fig. 6, it can be seen clearly that the pattern of compressive strength follows the pattern of CaO and Calcite content while $Fe_2O_3$ seems to no effect.

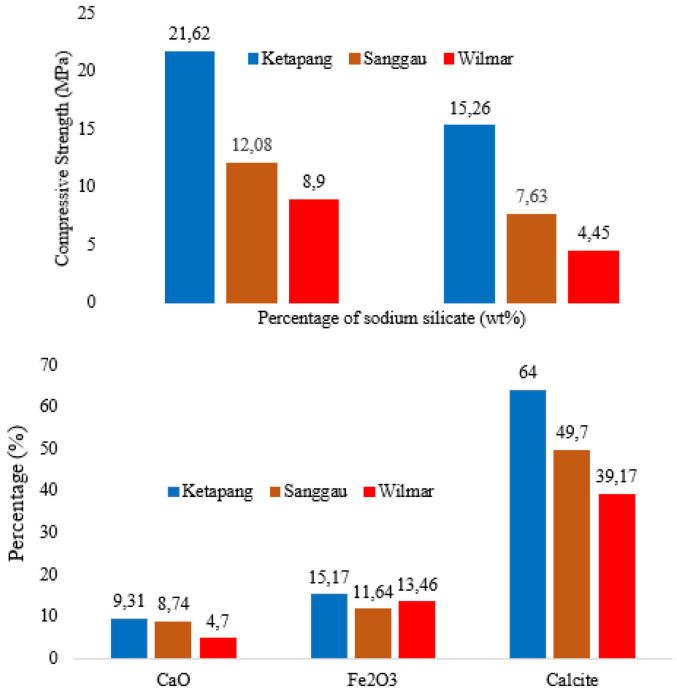


Fig. 6. Mechanical strength of geopolymer

## 4. Conclusions

1. Fly ash of Sanggau, Ketapang, and Wilmar with CaO content of 9.3, 8.7, and 4.7wt%, respectively were used as the raw materials for making geopolymers.
2. The three fly ashes were able to be made into geopolymer at the additions of 32 and 41wt%sodium silicate. The addition of 19wt% sodium silicate failed to produce geopolymer while the maximum compressive strength was achieved at the addition of 32wt% sodium silicate. The addition of higher sodium silicate than 32wt% resulted in lower compressive strength as well as longer setting time.
3. The compressive strength of the resulted geopolymers also follows the content of calcium and calcite content in the fly ash. The highest calcium and calcite content, the highest the compressive strength of the resulted geopolymer.
4. The geopolymer set longer when the sodium silicate concentration increases. In contrast, the compressive strength of geopolymer decrease when using a higher sodium silicate percentage.

**Acknowledgments**

This work was financially supported by PDUPT from Ministry of research and technology, Indonesia, contract Number No.6/E/KPT/2019 date 19 February 2019 and No.5/E1/KP.PTNBH/2019 date 29 March 2019 and 906/PKS/ITS/2019 date 29 March 2019.

## REFERENCES

[1] Y. Zhang, R. Xiao, X. Jiang, W. Li, X. Zhu, B. Huang, J. Cleaner. Prod. 273, 122970 (2020). DOI: https://doi.org/10.1016/j.jclepro.2020.122970

[2] İ.İ. Atabey, O. Karahan, C. Bilim, C.D. Atiş, Constr. Build. Mater. 264 (2020). DOI: https://doi.org/10.1016/j.conbuildmat.2020.120268

[3] C.L. Wong, K.H. Mo, U.J. Alengaram, S.P. Yap, J. Build. Eng. **32** 101655 (2020). DOI: https://doi.org/10.1016/j.jobe.2020.101655

[4] A. Abdullah, K. Hussin, M.M.A.B. Abdullah, Z. Yahya, W. Sochacki, R.A. Razak, K. Błoch, H. Fansuri, Materials **14**, 1111 (2021). DOI: https://doi.org/10.3390/ma14051111

[5] Y.S. Wang, Y. Alrefaei, J.G. Dai, Cem. Concr. Res. **127**, 105932 (2020). DOI: https://doi.org/10.1016/j.cemconres.2019.105932

[6] F. Demir, E. Moroydor Derun, J. Non-Cryst. Solids. **524**, 119649 (2019). DOI: https://doi.org/10.1016/j.jnoncrysol.2019.119649

[7] S. Top, H. Vapur, M. Altiner, D. Kaya, A. Ekicibil, J. Mol. Struct. 1202, 127236 (2020). DOI: https://doi.org/10.1016/j.molstruc.2019.127236

[8] O.H. Li, L. Yun-Ming, H. Cheng-Yong, R. Bayuaji, M.M.A.B. Abdullah, F.K. Loong, T.A. Jin, N.H. Teng, M. Nabiałek, B. Jeż, N.Y. Sing, Magnetochemistry **7** (1), 9 (2021). DOI: https://doi.org/10.3390/magnetochemistry7010009

[9] W.W.A. Zailani, M.M.A.B. Abdullah, M.F. Arshad, R.A. Razak, M.F.M. Tahir, R.R.M.A. Zainol, M. Nabialek, A.V. Sandu, J.J. Wysłocki, K. Błoch, Materials **14**, 56 (2021). DOI: https://doi.org/10.3390/ma14010056

[10] M.A. Faris, M.M.A.B. Abdullah, R. Muniandy, M.F. Abu Hashim, K. Błoch, B. Jeż, S. Garus, P. Palutkiewicz, N.A. Mohd Mortar, M.F. Ghazali, Materials **14**, 1310 (2021). DOI: https://doi.org/10.3390/ma14051310

[11] P. Zhang, Z. Gao, J. Wang, J. Guo, S. Hu, Y. Ling, J. Cleaner Prod. 270 122389 (2020). DOI: https://doi.org/10.1016/j.jclepro.2020.122389

[12] K.U. Ambikakumari Sanalkumar, M. Lahoti, E.H. Yang, Constr. Build. Mater. **225**, 283-291 (2019). DOI: https://doi.org/10.1016/j.conbuildmat.2019.07.140

[13] D. Panias, I.P. Giannopoulou, T. Perraki, Colloids Surf. A. **301**, 246-254 (2007). DOI: https://doi.org/10.1016/j.colsurfa.2006.12.064

[14] A.M. Kaja, A. Lazaro, Q.L. Yu, Constr. Build. Mater. **189**, 1113-1123 (2018). DOI: https://doi.org/10.1016/j.conbuildmat.2018.09.065

[15] M.N.S. Hadi, M. Al-Azzawi, T. Yu, Constr. Build. Mater. **175**, 41-54 (2018). DOI: https://doi.org/10.1016/j.conbuildmat.2018.04.092

[16] X.Y. Zhuang, L. Chen, S. Komarneni, C.H. Zhou, D.S. Tong, H.M. Yang, W.H. Yu, H. Wang, J. Cleaner Prod. **125**, 253-267 (2016). DOI: https://doi.org/10.1016/j.jclepro.2016.03.019.

[17] T. Hemalatha, A. Ramaswamy, J. Cleaner Prod. **147**, 546-559 (2017). DOI: https://doi.org/10.1016/j.jclepro.2017.01.114

[18] C. Belviso, Prog. Energy Combust. Sci. **65**, 109-135 (2018). DOI: https://doi.org/10.1016/j.pecs.2017.10.004

[19] R.E. Hidayati, G.R. Anindika, F.S. Faradila, C.I.B. Pamungkas, I. Hidayati, D. Prasetyoko, H. Fansuri, IOP Conf. Ser. Mater. Sci. Eng. Sci. Eng. **864** (2020). DOI: https://doi.org/10.1088/1757-899X/864/1/012017.

[20] J.G. Jang, H.K. Lee, Constr. Build. Mater. **102**, 260-269 (2016). DOI: https://doi.org/10.1016/j.conbuildmat.2015.10.172

[21] H. Fansuri, N. Swastika, L. Atmaja, Akta Kimindo **3**, 61-66 (2008).

[22] P. Rożek, M. Król, W. Mozgawa, Spectrochim. Acta – Part A. **198**, 283-289 (2018). DOI: https://doi.org/10.1016/j.saa.2018.03.034

[23] V. Gupta, D.K. Pathak, S. Siddique, R. Kumar, S. Chaudhary, Constr. Build. Mater. **235**, 117413 (2020). DOI: https://doi.org/10.1016/j.conbuildmat.2019.117413

[24] A. Mehta, R. Siddique, Constr. Build. Mater. **150**, 792-807 (2017). DOI: https://doi.org/10.1016/j.conbuildmat.2017.06.067.

[25] S.K. Nath, S. Kumar, Constr. Build. Mater. **233**, 117294 (2020). DOI: https://doi.org/10.1016/j.conbuildmat.2019.117294

[26] A. De Rossi, M.J. Ribeiro, J.A. Labrincha, R.M. Novais, D. Hotza, R.F.P.M. Moreira, Process Saf. Environ. Prot. **129**, 130-137 (2019). DOI: https://doi.org/10.1016/j.psep.2019.06.026

[27] L.N. Assi, E. Eddie Deaver, P. Ziehl, Constr. Build. Mater. **167**, 372-380 (2018). DOI: https://doi.org/10.1016/j.conbuildmat.2018.01.193

[28] D.-W. Zhang, D. Wang, Z. Liu, F. Xie, Constr. Build. Mater. **187**, 674-680 (2018). DOI: https://doi.org/10.1016/j.conbuildmat.2018.07.205

[29] P. Risdanareni, P. Puspitasari, E. Januarti Jaya, MATEC Web Conf. 97 (2017). DOI: https://doi.org/10.1051/matecconf/20179701031

[30] B.G. Kutchko, A.G. Kim, Fuel. **85**, 2537-2544 (2006). DOI: https://doi.org/10.1016/j.fuel.2006.05.016

[31] W.W.A. Zailani, A. Bouaissi, M.M. Al Bakri Abdullah, R. Abd Razak, S. Yoriya, M.A.A. Mohd Salleh, M.A.Z. Mohd Remy Rozainy, H. Fansuri, Appl. Sci. **10**, 1-14 (2020). DOI: https://doi.org/10.3390/app10093321

[32] D.D. Burduhos Nergis, P. Vizureanu, L. Andrusca, D. Achitei, IOP Conference Series: Materials Science and Engineering. **572**, 012026 (2019). DOI: https://doi.org/10.1088/1757-899X/572/1/012026

[33] D.D. Burduhos Nergis, P. Vizureanu, I. Ardelean, A.V. Sandu, O. Corbu, E. Matei, Materials **13**, 3211 (2020). DOI: https://doi.org/10.3390/ma13020343

[34] D.W. Zhang, D.M. Wang, F.Z. Xie, Constr. Build. Mater. **207**, 284-290 (2019). DOI: https://doi.org/10.1016/j.conbuildmat.2019.02.149

[35] L.H. Buruberri, D.M. Tobaldi, A. Caetano, M.P. Seabra, J.A. Labrincha, Elsevier Ltd, 2019. DOI: https://doi.org/10.1016/j.jobe.2018.11.017

[36] H. Fansuri, D. Prasetyoko, Z. Zhang, D. Zhang, Asia-Pac. J. Chem. Eng. **7** (1), 73-79 (2012). DOI: https://doi.org/10.1002/apj.493